

1 **Temporal and spatial patterns of internal and external stem CO₂ fluxes in a sub-**
2 **Mediterranean oak**

3 ROBERTO SALOMÓN¹, MARÍA VALBUENA-CARABAÑA¹, LUIS GIL¹, MARY
4 ANNE MCGUIRE², ROBERT TESKEY², DOUG AUBREY^{2,3}, INÉS GONZÁLEZ-
5 DONCEL¹, JESÚS RODRÍGUEZ-CALCERRADA¹

6

7 ¹ Forest Genetics and Ecophysiology Research Group, E.T.S. Forestry Engineering,
8 Technical University of Madrid, Ciudad Universitaria s/n, 28040, Madrid, Spain

9 ² Warnell School of Forestry and Natural Resources, University of Georgia, 180 East
10 Green St, Athens, GA. 30602-2152, USA

11 ³ Savannah River Ecology Lab, University of Georgia, Drawer E, Aiken, SC. 29802,
12 USA

13

14 Corresponding author: Jesús Rodríguez-Calcerrada

15 Tel.: +34913367113; Fax: +34 913572293; E-mail address: jesus.rcalcerrada@upm.es

16

17 **Key words**

18 carbon balance, daytime CO₂ depression, summer drought, forest decline, seasonal
19 variation, stem CO₂ efflux, carbon loss, xylem CO₂ transport

20 **Running head**

21 INTERNAL AND EXTERNAL STEM CO₂ FLUXES

22

23 **Summary**

24 To accurately estimate stem respiration (R_S), measurements of both CO₂ efflux to the
25 atmosphere (E_A) and internal CO₂ flux through xylem (F_T) are needed because xylem
26 sap transports respired CO₂ upward. However, studies of seasonal dynamics of F_T and
27 E_A are scarce and are non-existent in Mediterranean species under drought stress
28 conditions. Internal and external CO₂ fluxes at three stem heights, together with stem
29 growth, temperature, sap flow, and water potential were measured in *Quercus pyrenaica*
30 Willd. in four measurement campaigns during one growing season. Low internal [CO₂]
31 (<0.5%) resulted in low contributions of F_T to R_S throughout the growing season. R_S
32 was mainly explained by E_A (>90%), which varied seasonally, mirroring trends in sap
33 flow and stem growth. Nevertheless, at midday, when sap flow was high, F_T accounted
34 for up to 25% of R_S . Internal [CO₂] was also found to vary vertically along the stems
35 and in relation to root biomass among stems. Seasonality in xylem [CO₂] and resistance
36 to radial CO₂ diffusion was related to drought stress. Enhanced radial diffusion of CO₂
37 through cambium, phloem, and bark tissues due to water deficit, together with down-
38 regulation of xylem respiration ascribed to historical coppicing in Mediterranean stands,
39 may underpin low internal [CO₂] and F_T . Long term studies analyzing temporal and
40 spatial variation in internal and external CO₂ fluxes and their interactions are needed to
41 comprehensively understand and model respiration of woody tissues.

42 **Introduction**

43 Ecosystem respiration consumes 30-70% of carbon assimilated by photosynthesis
44 (Waring et al. 1998, Amthor 2000, Acosta et al. 2008, Ryan et al. 2009). Among
45 terrestrial ecosystems, CO₂ released by respiration of forests is a large component of the
46 global carbon budget, yet knowledge of respiratory processes, particularly woody tissue
47 respiration, is limited, especially in comparison to our understanding of photosynthesis
48 (Ryan et al. 2009, Guidolotti et al. 2013, Rambal et al. 2014). Stem respiration (R_S) has
49 been estimated to contribute 5 to 40% of total forest ecosystem respiration, depending
50 on forest type and season (Rodríguez-Calcerrada et al. 2014). Yet the abiotic and biotic
51 factors controlling R_S and contributing to its temporal and spatial variability remain
52 unclear.

53 To study variability in R_S , stem CO₂ efflux to the atmosphere (E_A) has been commonly
54 assumed to equal R_S (Stockfors and Linder 1998, Damesin et al. 2002, Lavigne et al.
55 2004, Acosta et al. 2008, Brito et al. 2010, Yang et al. 2012, Tarvainen et al. 2014,
56 Rodríguez-Calcerrada et al. 2015). However, in the last decade it has been demonstrated
57 that internal fluxes of CO₂ in stems play an important role in estimating woody tissue
58 respiration, since a portion of the CO₂ released by respiration dissolves in sap and is
59 transported upward in the xylem stream. Measurements of E_A have generally
60 underestimated respiration (Teskey et al. 2008, Hölttä and Kolari 2009, Angert et al.
61 2012, Trumbore et al. 2013, Bloemen et al. 2015), although CO₂ movement from the
62 roots upward can also result in overestimation (Zach et al. 2010, Bužková et al. 2015).
63 Using a mass balance approach, McGuire and Teskey (2004) revealed significant mis-
64 estimation of R_S by measurements of E_A and the absence of a consistent relationship
65 between R_S and E_A (Teskey and McGuire 2007). Briefly, the mass balance approach
66 considers the sum of three respiration components in a stem segment to estimate total
67 respiration on a volume basis. R_S components are: (i) E_A ; (ii) internal flux of dissolved
68 CO₂ through the xylem (F_T); and (iii) the change in CO₂ concentration ($[CO_2]$) (i.e. CO₂
69 stored in the stem segment) across two consecutive measurements (ΔS). The mass
70 balance approach has demonstrated that relative contributions of F_T to total R_S can be
71 highly variable, ranging from 3% to 55% for poplar and sycamore trees, respectively
72 (McGuire and Teskey 2004, Saveyn et al. 2008). From measurements of the ratio of
73 CO₂ efflux to O₂ influx, Angert *et al.* (2012) estimated that 35% of locally respired CO₂
74 was transported upward. The relevance of F_T to forest carbon budgets was noted by

75 Aubrey and Teskey (2009), who reported that the amount of CO₂ transported from roots
76 into the stem was of the same magnitude as soil CO₂ efflux in a poplar plantation. On
77 the contrary, internal CO₂ transport had no apparent effect on CO₂ efflux in large conifer
78 trees (Ubierna et al. 2009), or young pine trees during springtime (Maier and Clinton
79 2006). It is becoming apparent that internal [CO₂] measurements are necessary to better
80 integrate physiological processes at the cellular level with CO₂ fluxes from stem
81 surfaces (Trumbore et al. 2013), and to more accurately estimate R_S (McGuire and
82 Teskey 2004).

83 Previous research on R_S has revealed interesting interactions among F_T , E_A and internal
84 [CO₂]. For instance, increased F_T during daytime is associated with lower E_A . Daytime
85 depressions in E_A compared to nighttime values at the same temperature have been
86 attributed to transport of locally respired CO₂ (Bowman et al. 2005, Gansert and
87 Burgdorf 2005, Hölttä and Kolari 2009), even though direct assessments of upward
88 transport of CO₂ are typically missing in these studies. Moreover, [CO₂] has been shown
89 to be directly related to E_A (Teskey and McGuire 2002, 2007, Cerasoli et al. 2009), with
90 the slope of this relationship determining the resistance to radial diffusion of CO₂
91 (Steppe et al. 2007, Teskey et al. 2008). Resistance to radial CO₂ diffusion is dependent
92 on stem water status, tissue properties, and temperature (Nobel 1999). Diffusion
93 resistance influences the quantity of internal CO₂ that diffuses to the atmosphere
94 through cambium, phloem and bark tissues, and it could help explain the substantial
95 variation in CO₂ efflux observed among and within trees and across stands (Steppe et al.
96 2007).

97 Spatial and temporal changes in physical and biological factors underpin changes in R_S
98 and its components. For instance, vertical position on the stem is a significant factor
99 affecting CO₂ concentration and fluxes. A positive relationship between E_A and height
100 has been observed, presumably due to higher growth rates in the upper stem and tree
101 crown (Damesin et al. 2002, Araki et al. 2010, Tarvainen et al. 2014). In parallel, a
102 slightly increasing vertical gradient in [CO₂] was also observed from stem base to 3 m
103 height (Teskey and McGuire 2007), and Hölttä and Kolari (2009) modeled higher ratios
104 of CO₂ efflux to CO₂ production in the upper stem as CO₂ is transported upward.
105 Internal [CO₂] and CO₂ fluxes, especially at the stem base, could also be affected by the
106 influence of the extent and structure of the supporting root system on internal CO₂

107 transport from below ground (Teskey and McGuire 2007), which has never been
108 examined in natural conditions.

109 E_A varies seasonally, driven by abiotic factors such as temperature and water
110 availability, and biotic processes such as photosynthesis, phloem transport, and cambial
111 activity. Previous work based on E_A measurements has suggested that summer drought
112 reduces respiration (Maseyk et al. 2008, Brito et al. 2010, Rodríguez-Calcerrada et al.
113 2014). $[CO_2]$ and F_T might also vary seasonally, however, data on E_A , and more so
114 internal $[CO_2]$ and F_T , are scarce in drought-prone regions (but see Cerasoli *et al.*,
115 2009). Concomitant studies of E_A and $[CO_2]$ have rarely lasted more than two weeks
116 (see review by Teskey *et al.*, 2008). To date, the only published data in which both
117 internal and external CO_2 fluxes have been simultaneously monitored in a long term
118 experiment consists of measurements on two Norway spruce trees instrumented for 19
119 months (Etzold et al. 2013). This study revealed a close link between internal $[CO_2]$ and
120 both temperature and cambial activity.

121 Here, we aim to assess the main drivers of diel, seasonal, and vertical variability of E_A ,
122 internal $[CO_2]$, R_S , and their interactions in a sub-Mediterranean tree species (*Quercus*
123 *pyrenaica* Willd.) traditionally coppiced and currently abandoned. Variables E_A , F_T , and
124 internal $[CO_2]$ were examined at three different stem heights during the 2013 growing
125 season on four dates with contrasting sap flow rates, drought stress, and growth rates.
126 First, we examined variation in E_A across the growing season, and the effect of sap flow
127 and F_T on the widely reported daytime depression in E_A . We predicted that annual peak
128 E_A would occur at the beginning of the growing season, when water availability and
129 early-wood formation are highest, and that E_A would decrease over the course of the
130 growing season in response to drought and reduced growth. We also predicted
131 increasing daytime depression in E_A with increasing sap flow rate driven by the dilution
132 of $[CO_2^*]$ in the stem with water coming from the soil at relatively low $[CO_2^*]$, or with
133 drought severity as water limitation causes loss in cell turgor reducing respiration rates.
134 Second, we examined seasonal variation in internal $[CO_2]$ and how its relationship with
135 E_A (i.e. the resistance to radial CO_2 diffusion) changes as drought stress increases. We
136 expected that $[CO_2]$ would follow a similar pattern to E_A in response to cambial activity,
137 and that resistance to radial CO_2 diffusion would decline as water deficit increased.
138 Third, we calculated the contribution of F_T to R_S across the growing season and at
139 different stem heights. Using the mass balance approach proposed by McGuire and

140 Teskey (2004), we hypothesized that the contribution of F_T to R_S would be greater in the
141 middle of the growing season, coinciding with high sap flow rates, as well as at higher
142 stem positions, due to the buildup of CO_2 along the stem. Fourth, we examined the
143 relationship between internal $[\text{CO}_2]$ and root properties (living biomass and root
144 connections), with the expectation of higher $[\text{CO}_2]$ in stems supported by larger root
145 systems.

146 **Materials and Methods**

147 *Experimental plot and set-up*

148 The study was performed in a pure stand of *Q. pyrenaica* at the core of the species
149 distribution in the Central Mountain Range of the Iberian Peninsula. *Q. pyrenaica* is a
150 marcescent oak found in siliceous sub-Mediterranean mountains. Due to its high root-
151 resprouting capability, the species has been historically coppiced, leading to
152 anthropogenic ecosystems which physiognomy, functionality and ecology have been
153 altered (Valbuena-Carabaña and Gil 2013). The study plot was located in the buffer
154 zone of the national Park of “Sierra de Guadarrama”, in the “Monte Matas de Valsáin”,
155 at an altitude of 1140 m.a.s.l. Average annual rainfall and temperature were 885 mm and
156 10°C , respectively. Soil type is humic cambisol. The stand has been traditionally
157 coppiced but was abandoned after 1970, when the last cutting was performed. Stem
158 density was $781 \text{ stems ha}^{-1}$, with most of the stems ranging from 15 to 25 cm diameter
159 at breast height.

160 Eight stems were instrumented to measure internal and external CO_2 fluxes at their
161 base. All stems were part to the same clone. Only one clone was used because we
162 planned to excavate the root system of the entire multi-stemmed clone to link stem
163 $[\text{CO}_2]$ with root properties. For detailed methodology on clonal assignment see
164 Valbuena-Carabaña et al. (2008). Diameter at breast height (dbh) of the eight stems
165 ranged from 12.4 to 23.9 cm, and total height from 10.5 to 13.8 m. Four measurement
166 campaigns were made during the growing season of 2013. On each measurement date
167 we completed 24 hours of measurements, starting and finishing at approximately 12:00
168 h. The first measurement date, (D1), was on DOY 143-144 (end of May), during bud-
169 burst, when sap flow was negligible. The second and third measurement dates (D2 and
170 D3) were on DOYs 183-184 (beginning of July) and 218-219 (beginning of August),
171 respectively, with warmer temperatures and higher sap flow rates. Finally, D4 was on

172 DOY 266-267 (end of September) when transpiration was reduced, stem growth had
173 ceased, and drought stress, indicated by shoot water potential, was maximum (Figure 1).

174 Stem harvest and root excavation started on DOY 280. Stems were felled to quantify
175 sapwood volume per stem segment to calculate R_S by the mass balance approach (see
176 below). The root system was hydraulically excavated with a high-pressure water pump
177 down to 1m depth. Root connections were then quantified and categorized as parent
178 roots, from which stems sprout, and root grafts, formed after stem sprouting
179 (DesRochers and Lieffers 2001). The cross section of each root connection (cm^2) was
180 measured at the midpoint between connected stems (in the case of parental roots), or
181 estimated from two perpendicular diameters at each graft side (considering the smallest
182 root within the graft). After these measurements were complete, the root system was
183 lifted with a backhoe, coarse and taproots were separated and all roots were weighed on
184 a balance (BMM-BR80, Baxtran, Spain) *in situ* to the nearest 20 g.

185 *Climatic conditions, diameter increment, and shoot water potential*

186 Air temperature (T_{air} , °C) and precipitation were monitored during the study every 30
187 minutes by a weather station located 2.1 km away from the plot. Diameter increment of
188 every stem was measured by dendrometer bands (DS20, GIS Iberica, Spain) placed at
189 1.3 m height and inspected ca. every two weeks. As a surrogate for tree water status,
190 shoot water potential was measured on every measurement date with a pressure
191 chamber (PMS Instrument Co., OR, USA) at predawn (between 04:00 and 06:00 h) and
192 midday (between 13:00 and 15:00 h).

193 *CO₂ efflux to the atmosphere (E_A)*

194 CO₂ efflux to the atmosphere was measured every six hours at the base (20 cm above
195 ground level) of each stem (at 12:00, 18:00, 00:00 and 06:00 h). Additionally, two stems
196 were intensively measured (18 times per day) at the base and two additional heights (1.5
197 m and 3 m). These two stems (S1 and S2) had dbh of 22.9 and 21.0 cm, respectively. E_A
198 was measured with a portable infrared gas analyzer (LI-6400, Li-Cor Inc., Lincoln, NE,
199 USA) and a soil chamber (LI-6400-09) as described in Xu *et al.*, (2000). Measurements
200 were made at the same stem location each time by fixing permanent PVC collars to the
201 stem. Loose bark was removed and the PVC collars were sanded to better fit stem
202 curvature. Silicone sealant and liquid rubber (Plasti-Dip, TRP, Spain) were applied to

203 prevent leaks. Measurements were made by reducing CO₂ concentration inside the
204 chamber and then letting it increase to an upper concentration limit (i.e., gas analyzer
205 operated in closed system configuration). These limits changed depending on the
206 respiration rate of the measured stem and the atmospheric [CO₂] concentration, which
207 averaged 370 ppm during the day and 420 ppm at night. The rate of change of [CO₂]
208 inside the chamber was calculated at ambient [CO₂] and humidity in three consecutive
209 measurement cycles. E_A values were corrected to account for stem collar volume, which
210 was measured at the end of the experiment by sealing the open end of the collar and
211 filling it with water through a hole in the top from a graduated cylinder. A correction
212 was applied to account for stem curvature using the equations developed by Xu *et al.*
213 (2000), so that E_A was calculated on stem surface area basis ($E_{A(S)}$ [$\mu\text{mol m}^{-2} \text{s}^{-1}$]).

214 Stem temperature (T_{stem} , °C) was continuously measured with type-T thermocouples
215 (copper-constantan) inserted at 2 cm depth and 5 cm away from each stem collar.

216 Temperature sensitivity of E_A (Q_{10}) was assessed by the equations:

$$217 \ln(E_A) = a + b T_{\text{stem}} \quad (1)$$

$$218 Q_{10} = e^{(b10)} \quad (2)$$

219 For comparison among measurement campaigns, $E_{A(S)}$ was standardized to 15°C
220 ($E_{A(S)15}$) – a temperature registered in all four campaigns and widely reported in
221 literature – using Q_{10} values obtained by pooling nighttime and daytime data.

222 To assess daytime depressions in efflux, residuals ($E_{A(S)\text{-RES}}$) were calculated in the
223 intensively measured stems (S1 and S2) as the difference between $E_{A(S)}$ predicted from
224 the nighttime relationship between T_{stem} and $E_{A(S)}$ (from 22:00 to 06:00 h) and measured
225 daytime $E_{A(S)}$.

226 *Internal [CO₂] and the mass balance approach*

227 Internal [CO₂] was measured at the base (10 cm above ground level) of the stems.
228 Additionally, in the intensively measured stems (S1 and S2), internal [CO₂] was
229 measured 5 cm above and below the stem collars (at 1.5 and 3 m height) to calculate
230 respiration by mass balance as proposed by McGuire and Teskey (2004). Internal [CO₂]
231 was measured with solid state non-dispersive infrared (NDIR) CO₂ sensors (model
232 GMM221, Vaisala, Finland) inserted into the stem. Holes of 40 mm length and 25 mm

233 width were drilled to place the sensor. NDIR sensors were isolated from the external
 234 atmosphere with rubber sealant. To minimize temperature effects associated with stem
 235 position stem collars, NDIR sensors and thermocouples were all oriented facing north to
 236 minimize effects of solar radiation (Stockfors and Linder 1998, Acosta et al. 2008).

237 NDIR sensors measure internal $[CO_2]$ in gaseous phase (%) in equilibrium with CO_2
 238 dissolved in sap solution ($[CO_2^*]$, $mmol L^{-1}$). Sap $[CO_2^*]$ is estimated by Henry's law
 239 from gas phase $[CO_2]$, sap temperature, and sap pH. Sap pH was measured at midday, at
 240 maximum transpiration rates, using a portable pH meter (model 25+, Crison, Barcelona)
 241 and a pH electrode (model 52 07, Crison, Barcelona) on sap expressed from twigs of
 242 each stem. To measure sap flux density ($L cm^{-2} h^{-1}$), two thermal dissipation probes
 243 (Granier 1985) were inserted to a depth of 2 cm into the sapwood on opposite sides of
 244 each stem (west and east oriented) at 1 m height. The paired needles of each probe were
 245 separated 10 cm vertically. Daily zero flow was calculated for each probe from the
 246 temporal mean of the temperature difference of the thermocouple pair between 04:00
 247 and 06:00 h. Data from the two probes per stem were averaged to account for
 248 circumferential variability in sap flux. Calibration parameters developed by Sun *et al.*
 249 (2011) were applied to sap flux density to improve accuracy according to the ring
 250 porous xylem anatomy of *Q. pyrenaica* stems. Sap flux density was multiplied by
 251 sapwood area to determine sap flow (F_{H_2O} , $L h^{-1}$). Stem temperature, sap flux density,
 252 and internal $[CO_2]$ were measured every minute and averaged every 15 minutes with a
 253 data logger (model CR23X, Campbell Scientific, Spain).

254 The mass balance approach was applied to calculate the relative contributions of E_A , F_T ,
 255 and ΔS to R_S following equations in McGuire and Teskey (2004):

$$256 \quad R_S = E_A + F_T + \Delta S \quad (3)$$

$$257 \quad F_T = (F_{H_2O}/V) \Delta[CO_2^*] \quad (4)$$

$$258 \quad \Delta S = ([CO_2^*]_{T1} - [CO_2^*]_{T0}) L/T \quad (5)$$

259 where R_S , E_A , F_T and ΔS are the stem respiration components on a volume basis (μmol
 260 $CO_2 m^{-3} s^{-1}$), F_{H_2O} is sap flux ($L s^{-1}$), V is sapwood volume of stem segment (m^3),
 261 $\Delta[CO_2^*]$ is the difference in sap $[CO_2^*]$ above and below the PVC collar, $[CO_2^*]_{Ti}$ is the
 262 mean of sap $[CO_2^*]$ above and below the collar at i -th time period, L is the stem water
 263 content ($L m^{-3}$), and T is the elapsed time (s) between consecutive measurements.

264 E_A was initially estimated on a stem surface area basis ($E_{A(S)}$). To express E_A on a
 265 volume basis ($E_{A(V)}$), we assumed uniform efflux around the stem circumference and
 266 used this equation:

$$267 \quad E_{A(V)} = E_{A(S)} \frac{S}{V} = E_{A(S)} \frac{2\pi r_{h+s} \text{height}}{\pi(r_{h+s}^2 - r_h^2) \text{height}} = E_{A(S)} \frac{2r_{h+s}}{(r_{h+s}^2 - r_h^2)} \quad (6)$$

268 where S and V are the axial surface area and volume of sapwood of the stem segment,
 269 respectively; r_h and r_{h+s} denote the radius of heartwood and heartwood plus sapwood,
 270 respectively; and height is the vertical length of the stem segment. The mass balance
 271 approach, on a sapwood volume basis, was applied on the four dates and at two heights
 272 (1.5 and 3 m) of the intensively measured stems (S1 and S2). However, in one stem
 273 segment (S2 at 3 meters) a NDIR probe failed on two sampling dates and these values
 274 were removed from analyses.

275 *Data analysis*

276 To study the influence of T_{stem} on diel E_A and internal $[\text{CO}_2]$, linear regressions were
 277 performed (Eq. 1). Seasonal differences in E_A and internal $[\text{CO}_2]$ at the stem base were
 278 assessed with hierarchical mixed models performed in R using the *lme* function in the
 279 nlme library (Pinheiro et al. 2015) considering measurement date as a fixed factor (n=4)
 280 and stem as a random factor (n=8). To evaluate the influence of stem height on E_A and
 281 $[\text{CO}_2]$, mixed models were performed considering date (n=4) and height (n=3) as fixed
 282 factors and stem (n=2, intensively measured stems S1 and S2) as a random factor.
 283 Backward selection was used to determine the most appropriate model until all
 284 variables included in the model were significant ($P < 0.05$). Multiple comparisons of
 285 means were performed using *glht* function in the multcomp library (Hothorn et al.
 286 2008).

287 To evaluate the influence of sap flow on daytime depression of efflux, mixed models
 288 were performed. At a diel scale (dates separately examined), $E_{A(S)_RES}$ ($\mu\text{mol CO}_2 \text{ m}^{-2} \text{ s}^{-1}$)
 289 was regressed against $F_{\text{H}_2\text{O}}$ (L h^{-1}) which was treated as a fixed factor, while stem
 290 segment nested within its corresponding stem (n = 2) was treated as a random factor. To
 291 test differences in slopes between $F_{\text{H}_2\text{O}}$ and $E_{A(S)_RES}$ among dates, ANCOVA was
 292 performed. At a seasonal scale, and to further distinguish between water status and
 293 internal CO_2 transport as potential drivers of daytime depression in efflux (Saveyn et al.
 294 2007a), daily accumulated $E_{A(S)_RES}$ ($\text{mmol CO}_2 \text{ m}^{-2} \text{ day}^{-1}$) was regressed against

295 accumulated F_{H_2O} (L day⁻¹) and predawn and midday shoot water potential (MPa)
296 considering the four measurement dates. Additionally, to estimate the portion of efflux
297 depression attributed to the internal transport of CO₂, the ratio between F_T and $E_{A(V)}_{RES}$
298 (on a volume basis, mmol CO₂ m⁻³ day⁻¹) was calculated for the four dates. According to
299 Fick's first law, the resistance to radial CO₂ diffusion (s m⁻¹) was calculated by the ratio
300 $\Delta[CO_2]/E_{A(S)}$, where $\Delta[CO_2]$ is the difference in [CO₂] ($\mu\text{mol m}^{-3}$) between the xylem
301 and the atmosphere (Steppe et al. 2007, Teskey et al. 2008). Resistance to radial CO₂
302 diffusion across dates was assessed with mixed models and differences among dates
303 were tested by ANCOVA. To evaluate the effect of root size and root connections on
304 internal [CO₂] at the stem base, average [CO₂] per stem was linearly regressed against
305 root variables. All values presented in the text are means \pm (SE).

306 **Results**

307 *Climatic conditions, water potential, and stem growth*

308 Over the growing season (from DOY 100 to 304), average T_{air} was 15.7 °C (daily means
309 ranged from 0.6 to 26.6 °C) and total precipitation was 214 mm, 60% of which occurred
310 before or during budburst (from DOY 140 to 150, Figure 1a). Summer was hot and dry:
311 from DOY 160 to 270, mean T_{air} was 19.7 °C (daily means ranged from 8.7 to 26.6 °C)
312 and total precipitation was 37.6 mm. Mean predawn and midday shoot water potential at
313 the end of the growing season (DOY 267) reached minimum values of -1.4 and -2.7
314 MPa, respectively. Stem growth started by DOY 110 and finished by DOY 260. Mean
315 accumulated diameter growth was 0.8 mm, of which 25% took place before and during
316 budburst (Figure 1b).

317 *Stem CO₂ efflux (E_A) and daytime depression in E_A*

318 $E_{A(S)}$ was strongly related to T_{stem} . On a diel basis, T_{stem} explained 82-97% of the
319 variability in $E_{A(S)}$ during the night (Table 1). The Q_{10} values were 1.85, 1.60, 1.76 and
320 1.99 for the four sampling periods, D1 to D4. Pooling nighttime and daytime data
321 reduced the number of significant relationships between T_{stem} and $E_{A(S)}$, as well as the
322 variability in $E_{A(S)}$ explained by T_{stem} (33-64%); the Q_{10} values decreased to 1.33, 1.30,
323 1.30 and 1.39 for the four sample periods, respectively.

324 Stem CO₂ efflux was standardized to 15°C ($E_{A(S)15}$) to examine the effect of season on
325 $E_{A(S)}$. For the four sampling periods $E_{A(S)15}$ varied significantly from 1.28 (0.14), 2.00

326 (0.27), 2.39 (0.36) and 1.65 (0.28) $\mu\text{mol CO}_2 \text{ m}^{-2} \text{ s}^{-1}$, for D1, D2, D3 and D4,
327 respectively ($n = 8$, $P < 0.001$), and every contrast examined among dates was
328 significant ($P < 0.05$). $E_{A(S)}$ at actual mean temperature on each date showed greater
329 differences: 1.09 (0.13), 2.18 (0.28), 2.76 (0.37) and 1.86 (0.27) $\mu\text{mol CO}_2 \text{ m}^{-2} \text{ s}^{-1}$,
330 measured at T_{stem} of 11.1 (0.2), 17.6 (0.2), 18.4 (0.1) and 18.9 (0.1) $^{\circ}\text{C}$, on the four
331 dates, respectively. In the stems measured at three heights (S1 and S2), $E_{A(S)15}$ was
332 marginally influenced by stem height ($P = 0.085$). Stem efflux ($E_{A(S)15}$) was similar at
333 the base of the stem and at 1.5 m height ($P = 0.744$), but at 3 m it was significantly
334 lower than at 1.5 m ($P = 0.027$) and tended to be lower than at the stem base ($P =$
335 0.059).

336 Hysteresis between diel T_{stem} and $E_{A(S)}$ was observed on all measurement dates, stems,
337 and heights; i.e., for a given temperature $E_{A(S)}$ was higher at nighttime than at daytime
338 (Figure 2). At a diel scale (dates separately examined), hysteresis ($E_{A(S)_RES}$, i.e.
339 predicted $E_{A(S)}$ - measured $E_{A(S)}$, $\mu\text{mol CO}_2 \text{ m}^{-2} \text{ s}^{-1}$) was related to F_{H2O} from D2 to D4,
340 which was the period in which transpiration occurred ($P < 0.001$, Figure 3). ANCOVA
341 showed that the slopes of these relationships were similar on D2 and D3 ($P = 0.378$),
342 whereas slopes on D2 and D3 were different than the slope on D4 ($P < 0.001$).
343 Interestingly, on D1, during budburst, hysteresis occurred in the absence of sap flow,
344 and $E_{A(S)_RES}$ was as large as on the dates with fully developed leaves (Figure 3).
345 Therefore, at a seasonal scale, daily accumulated $E_{A(S)_RES}$ ($\mu\text{mol CO}_2 \text{ m}^{-2} \text{ day}^{-1}$) per
346 measurement date was not influenced by daily accumulated sap flux ($\text{L m}^{-2} \text{ day}^{-1}$) ($P =$
347 0.525) but tended to increase with decreasing shoot water potential at predawn ($P =$
348 0.066) and midday ($P = 0.054$). Considering daily accumulated F_T (calculated by the
349 mass balance approach) and $E_{A(V)_RES}$ (both on a sapwood volume basis, $\text{mmol CO}_2 \text{ m}^{-3}$
350 day^{-1}), the mean ratio $F_T / E_{A(V)_RES}$ was -0.01 (0.01), 0.70 (0.23), 0.80 (0.26) and 0.49
351 (0.28) for dates D1 to D4, indicating that hysteresis in E_A was not fully explained by F_T ,
352 and not at all on D1 when transpiration was negligible.

353 *Internal [CO₂] and resistance to radial CO₂ diffusion*

354 Relationships between internal [CO₂] and T_{stem} at the base of the stem were
355 predominantly positive at night throughout the growing season, but pooling nighttime
356 and daytime data substantially reduced the number of significant positive relationships
357 between internal [CO₂] and T_{stem} (Table 1). The shifting pattern of this relationship

358 prevented us from estimating $[\text{CO}_2]$ at a reference temperature as we had done for E_A
359 using $E_{A(S)15}$. Internal $[\text{CO}_2]$ decreased over the growing season from 0.26 (0.06), 0.14
360 (0.03), 0.13 (0.02) to 0.11 (0.02)%, on D1, D2, D3, and D4, respectively ($P < 0.001$).

361 The ratio between $\Delta[\text{CO}_2]$ and $E_{A(S)}$, i.e. the resistance to radial CO_2 diffusion, changed
362 across the growing season (Figure 5). On D1, this resistance was the highest (1.08×10^5
363 $(3.63 \times 10^3) \text{ s m}^{-1}$), and a strong positive relationship between $\Delta[\text{CO}_2]$ and $E_{A(S)}$ was
364 found (average $R^2 = 0.96$, $P < 0.001$). On the remaining measurement dates, the
365 relationships between $\Delta[\text{CO}_2]$ and $E_{A(S)}$ were weaker: average R^2 values were 0.72 ,
366 0.19 and 0.66 for D2, D3 and D4 respectively. From D2 to D4, resistance to radial CO_2
367 diffusion was lower, decreasing by up to 1/4 compared to D1: 3.68×10^4 (2.07×10^3),
368 2.61×10^4 (6.98×10^3) and 3.85×10^4 (3.12×10^3) s m^{-1} , respectively ($P < 0.001$)
369 (Figure 5). The contrasts comparing slopes (i.e., resistance to radial CO_2 diffusion) by
370 ANCOVA were significant between D1 and all other dates ($P < 0.001$), but not among
371 D2, D3, and D4 ($P > 0.1$). Resistance to diffusion tended to decrease with decreasing
372 midday shoot water potential ($R^2 = 0.893$, $P = 0.055$, $n = 4$) but not with predawn shoot
373 water potential ($P = 0.924$, $n = 4$), suggesting that the resistance to diffusion was
374 influenced by midday water status.

375 Among the eight stems, the seasonal mean of internal $[\text{CO}_2]$ at the base of the stem was
376 positively related to taproot biomass ($P = 0.049$; $R^2 = 0.50$), and the accumulated cross
377 section of its root connections ($P = 0.027$; $R^2 = 0.58$). In the stems measured at three
378 heights (S1 and S2), internal $[\text{CO}_2]$ was influenced by date, height, and their interaction
379 ($P < 0.001$), varying from 0.52% (at 3 m height on D1) to 0.12% (at the stem base on
380 D2; Figure 4). Pooling dates, internal $[\text{CO}_2]$ increased from 0.17 (0.02)% at stem base,
381 to 0.26 (0.02)% at 1.5 m, and finally 0.40 (0.02)% at 3 m height ($P < 0.001$).

382 *Components of stem respiration by a mass balance approach*

383 Daily values of R_S and its components ($E_{A(V)}$, F_T , and ΔS), as well as their proportional
384 contributions to R_S , varied with date, stem, and stem height (Table 2; Figure 6). The
385 lowest R_S , 4.69 (0.37) $\text{mol m}^{-3} \text{ day}^{-1}$, was found on D1; and R_S increased to 13.68
386 (0.86), 13.94 (0.63) and 13.75 (2.30) $\text{mol m}^{-3} \text{ day}^{-1}$ on consecutive subsequent dates.
387 The contribution of ΔS to R_S was always negligible, with daily contributions ranging
388 from -0.4 to 0.1%. However, a linear model testing the contribution of F_T to R_S by date
389 and height showed that F_T contributions changed significantly across the growing

390 season ($P = 0.046$) and also changed marginally with stem height ($P = 0.071$). The
391 average contribution of F_T to R_S was nil at D1 due to negligible transpiration and
392 increased to 5 - 6.5% on the remaining dates ($P = 0.046$), among which no significant
393 differences were found ($P > 0.1$). The contribution of F_T to R_S tended to be 3.3% larger
394 at 3 m compared to 1.5 m height ($P = 0.071$). $E_{A(V)}$ was the main component of daily R_S ,
395 with contributions above 90% in most cases (Table 2). At a diel scale, the contribution
396 of $E_{A(V)}$ to R_S was close to 100% at night (Figure 6). In the daytime, the contribution of
397 $E_{A(V)}$ to R_S declined (in some cases to 75%) at high sap flow rates, when the
398 contribution of F_T to R_S reached maximum values close to 25% (Figure 6a).

399 Discussion

400 *Stem CO₂ efflux (E_A) and daytime depression in E_A across the season*

401 Stem CO₂ efflux varied from 1.28 to 2.39 $\mu\text{mol CO}_2 \text{ m}^{-2} \text{ s}^{-1}$ at a reference temperature
402 of 15°C, which is within the range of values reported for different *Quercus* species
403 (Edwards and Hanson 1996, Saveyn et al. 2007a, 2007b, Yang et al. 2012, Rodríguez-
404 Calcerrada et al. 2014, 2015). In agreement with data from Barbaroux and Bréda
405 (2002), Corcuera et al. (2006) and Courty et al. (2007), accumulated stem diameter
406 increment before and during budburst accounted for one fourth of total annual stem
407 diameter increment. Thus, we expected high $E_{A(S)15}$ at the beginning of the growing
408 season, driven by the absence of drought stress and high rates of wood production
409 (Lavigne et al. 2004). However, $E_{A(S)15}$ was lowest on D1. Negligible respiration of
410 phloem tissues (Amthor 2000) and no supply of new assimilates (Wertin and Teskey
411 2008, Maier et al. 2010) may result in low $E_{A(S)15}$ before leaf expansion. $E_{A(S)15}$ showed
412 maximum values in mid-summer (D2 and D3), coinciding with maximum transpiration
413 and high stem growth (e.g. Damesin et al., 2002; Acosta et al., 2008; Yang et al. 2012;
414 Guidolotti et al., 2013; Tarvainen et al., 2014). The decrease in $E_{A(S)15}$ at the end of the
415 growing season (D4) could be explained by stem growth cessation and reduced water
416 availability (Figure 1b). Yet, contrary to other studies in drier Mediterranean regions
417 (Maseyk et al. 2008, Brito et al. 2010, Rodríguez-Calcerrada et al. 2014), mild drought
418 stress (with minimum predawn shoot water potential of -1.4 MPa) did not result in large
419 reductions of $E_{A(S)15}$ in our study.

420 We hypothesized that E_A would increase with height due to increased metabolic activity
421 (Damesin et al. 2002, Araki et al. 2010, Tarvainen et al. 2014) and internal upward

422 movement of CO₂ (Hölttä and Kolari 2009). However, stem height barely affected
423 $E_{A(S)15}$. The short vertical gradient (3 m) and the fact that the highest sampling point was
424 below the tree crown may have contributed to the limited spatial variability observed in
425 $E_{A(S)15}$.

426 Sap flow was a reliable predictor of depression in daytime CO₂ efflux (Bowman et al.
427 2005, Gansert and Burgdorf 2005, Hölttä and Kolari 2009), but only after leaf
428 expansion (from D2 to D4, Figure 3). The ratio between F_T and $E_{A(V)_RES}$ ranging from
429 0.49 to 0.80 from D2 to D4 suggests that 50% or more of the hysteresis in $E_{A(V)}$ could
430 be attributed to the internal transport of CO₂ after leaf expansion. However,
431 measurements on D1 during budburst, when hysteresis in $E_{A(S)}$ could not be ascribed to
432 transpiration, showed $E_{A(S)_RES}$ as large as after leaf expansion (Figure 3), suggesting
433 that transpiration is not the only process determining daytime depression in $E_{A(S)}$
434 (Saveyn et al. 2007a). Similarly, Etzold *et al.* (2013) found that relationships between
435 depressions in $E_{A(S)}$ and sap flow in Norway spruce trees were significant only during
436 the growing period. The inverse relationship ($P < 0.1$) between daily accumulated
437 $E_{A(S)_RES}$ and shoot water potential observed in this study reinforces the suggestion of
438 Saveyn *et al.*, (2007a) that low water availability and low turgor pressure limit
439 respiration and elicit a depression in $E_{A(S)}$ during daytime.

440 *Internal [CO₂] and its relationship to E_A (resistance to radial CO₂ diffusion)*

441 Internal [CO₂] varied between 0.11 and 0.52%. These values were an order of
442 magnitude lower than those generally observed using this methodology. However,
443 internal [CO₂] lower than 0.5% was also observed for several species using different
444 methodologies (see Table 1 in Teskey *et al.*, 2008), and at this site during the 2012
445 growing season (Salomón et al. 2015). Comparatively low xylem [CO₂] and $E_{A(S)}$
446 similar to commonly reported rates might be explained by the combination of low
447 respiration of xylem living cells and high radial diffusion of CO₂. First, low xylem
448 respiration in roots and stems can be attributed to the over-aged status of trees in this
449 historically coppiced stand (Manuel Valdés and Rojo y Alboreca 1993). Limited growth
450 (Figure 1b, Corcuera et al. 2006, Salomón et al. 2013) and low proportion of sapwood
451 (mean sapwood thickness was 2.5 cm) in over-aged stems relative to trees in other
452 experiments using this methodology might result in comparatively low respiration rates
453 of xylem tissues. The reduction in carbon expenditures by an acclimation of respiration

454 may enhance carbohydrate storage to support resprouting (Zeppel et al. 2015), the
455 reproductive strategy of this species. Second, limited water availability in drought-prone
456 regions may have a key role explaining the amount of respired CO₂ that built up in roots
457 and stems or diffused to the soil and atmosphere. Gas diffusion is much higher (~10⁴) in
458 gas than in water (Nobel 1999). Thus, progressive soil drying across the growing season
459 might have resulted in a progressively larger proportion of root-respired CO₂ diffusing
460 through soil to the atmosphere relative to the amount dissolving in sap solution and
461 moving upward in the transpiration stream. Consistently, F_T as low as 2% of the root-
462 respired CO₂ that diffused through soil to the atmosphere has been observed at this
463 experimental site (Salomón et al. 2015), which likely decreased the [CO₂] at the base of
464 the stem relative to that measured in other studies (e.g. Aubrey and Teskey 2009). This
465 is the first study in which [CO₂] was measured in a sub-Mediterranean species during
466 the dry season. To date, [CO₂] has been monitored in temperate and boreal species
467 where water availability is not a limiting factor for stem respiration. In the only
468 manipulative drought experiment using this methodology, values as low as 0.3 mmol L⁻¹
469 ($\approx 0.3\%$ in the gaseous phase assuming $T_{\text{stem}} = 15^\circ\text{C}$ and sap pH = 6.5) were observed in
470 *Q. robur* trees at higher midday water potential than in this study (Saveyn et al. 2007b).
471 In support of this idea, it is worth noting that in the same experimental site, [CO₂]
472 exhibited a 20-fold increase after a heavy rain at the end of the dry season (manuscript
473 in prep.), similar to observations by Saveyn et al. (2007b) after rewatering. Furthermore,
474 due to the steep decline in latewood formation in over-aged stems of *Q. pyrenaica*
475 (Corcuera et al. 2006), the high proportion of large early-wood vessels may facilitate the
476 radial diffusion of respired CO₂ (Soriz and Hietz 2006).

477 Our observation that [CO₂] was highest on D1 compared with the other dates was most
478 likely due to the absence of [CO₂] dilution by transpiration on D1 (Teskey and McGuire
479 2002), but increasing drought and healing of wounds caused by CO₂ sensor installation
480 (see Etzold et al. 2013) could have also contributed to the decline in [CO₂] over the
481 growing season. Additionally, enhanced cambial activity due to primary root elongation
482 (Courty et al. 2007) and early-wood formation in *Q. pyrenaica* branches (Corcuera et al.
483 2006) during spring may have also increased [CO₂] at the stem base and at 3 m,
484 respectively, compared with measurements later in the season (Figure 4). This pattern of
485 [CO₂] did not hold at 1.5 m, which was similar to the date-by-height interaction
486 observed in a pioneering study of stem [CO₂] (Chase 1934). In any case, pooled data

487 showed an increasing vertical gradient in [CO₂], suggesting that respired CO₂ was
488 transported upward (Teskey and McGuire 2007, Hölttä and Kolari 2009).

489 Recent work has provided interesting data on the amount of CO₂ that moves from the
490 roots upward (Bloemen et al. 2015), but there are still challenging issues regarding
491 internal CO₂ transport, such as the effect of root structure on internal [CO₂]. Multi-
492 stemmed trees offer a good opportunity to study how root-respired CO₂ moves
493 horizontally through roots and upward into stems. Here we found that stems supplied by
494 larger taproots connected to greater amounts of belowground biomass had higher [CO₂]
495 at the base than those connected to fewer and smaller roots. This possibility was
496 suggested by Teskey & McGuire (2007) and has found empirical support here, in
497 natural conditions. It provides a new evidence of the difficulty in ascribing stem CO₂
498 efflux to the respiration rate of directly adjacent cells.

499 Seasonal variability in the resistance to radial CO₂ diffusion is another overlooked
500 factor that could help to comprehensively understand and model stem respiration.
501 Resistance to radial CO₂ diffusion determines the fate of locally respired CO₂ by
502 changing the potential for CO₂ to diffuse outward and contribute to $E_{A(S)}$ or
503 alternatively, to accumulate and dissolve in xylem sap and contribute to F_T . Resistance
504 to radial diffusion of CO₂ was estimated from the relationship between internal [CO₂]
505 and $E_{A(S)}$ (Steppe et al. 2007, Teskey et al. 2008). Although no relationship between
506 [CO₂] and $E_{A(S)}$ has been found in some studies (see Maier & Clinton, 2006 and Saveyn
507 *et al.*, 2007b), here, a strong direct relationship between internal [CO₂] and $E_{A(S)}$ was
508 found on D1 during budburst ($R^2 = 0.96$, $P < 0.001$) and, similar to findings of Saveyn
509 *et al.* (2007b), the strength of the relationship diminished during the dry season. In
510 addition to affecting the rate of respiration, seasonal changes in temperature and water
511 availability also alter the relative volume of gas and water in stems, and thus influence
512 stem permeability to CO₂ (Nobel 1999). In our study, resistance to radial CO₂ diffusion
513 was 3-4 times higher on D1 than D2, D3 or D4. Similarly, Fick's radial diffusion
514 coefficient increased 5- fold in *Q. robur* when gas volume increased (to the detriment of
515 water volume) from 15 to 40% (Sorz and Hietz 2006). The direct relationship between
516 the resistance to radial CO₂ diffusion and midday water potential ($R^2 = 0.89$, $P = 0.06$)
517 suggests that greater drought stress concomitantly reduced stem water content and the
518 resistance to radial CO₂ diffusion. Low resistance to radial diffusion after leaf expansion

519 (from D2 to D4) might be an underlying cause of the low contribution of F_T to R_S
520 observed during dates of substantial transpiration (see below).

521 *Seasonal dynamics of stem respiration and its contributors*

522 Stem respiration (R_S) was calculated by the mass balance approach proposed by
523 McGuire and Teskey (2004), which elucidated the contributions of $E_{A(V)}$, F_T , and ΔS to
524 R_S . Average R_S on D1 was $4.7 \text{ mol m}^{-3} \text{ day}^{-1}$, and increased to 13.7, 13.9, and 13.8 mol
525 $\text{m}^{-3} \text{ day}^{-1}$ on D2, D3, and D4, respectively. Values of R_S were similar to the range of
526 reported values applying this methodology: $3.3 \text{ mol m}^{-3} \text{ day}^{-1}$ for *Dacrydium*
527 *cupressinum* trees (Bowman et al. 2005); $5.1 \text{ mol m}^{-3} \text{ day}^{-1}$ for *P. occidentalis* trees
528 (calculated from Teskey & McGuire, 2007); 7.4, 5.8 and $4.2 \text{ mol m}^{-3} \text{ day}^{-1}$ for *Fagus*
529 *grandifolia*, *Platanus occidentalis* and *Liquidambar styraciflua*, respectively (McGuire
530 and Teskey 2004); and from 21.3 to $49.5 \text{ mol m}^{-3} \text{ day}^{-1}$ in young *Populus deltoides* trees
531 (Saveyn et al. 2008). The contribution of ΔS to R_S was negligible, ranging from -0.4 to
532 0%, which was consistent with previous studies. Thus F_T , and particularly E_A , were the
533 main contributors to R_S . The contribution of F_T during budburst was nil and then
534 increased to an average of only 5 - 6.5% of R_S after leaf expansion. This contribution is
535 in the lower range of reported values: 3 - 18 % for *P. deltoides* trees (Saveyn et al.
536 2008); 10.6% for *D. cupressinum* trees (Bowman et al. 2005); 14% for *F. grandifolia*
537 and 15% for *L. styraciflua* (McGuire and Teskey 2004); and 34 % and 55% for *P.*
538 *occidentalis* at different times (McGuire and Teskey 2004, Teskey and McGuire 2007).
539 Although $[\text{CO}_2]$ in *Q. pyrenaica* stems was an order of magnitude lower than in
540 previous studies, the contribution of F_T to R_S was within the same order of magnitude.
541 This apparently counterintuitive observation is explained by the fact that F_T is not
542 proportional to the absolute internal $[\text{CO}_2]$, since F_T is directly calculated from the
543 difference in dissolved $[\text{CO}_2^*]$ between two stem points (here separated by 25 cm; Eq.
544 4).

545 The only significant variation in the contribution of F_T to R_S across the growing season
546 was explained by the resumption of transpiration that occurred between D1 and D2.
547 After leaf expansion (from D2 to D4) the contribution of F_T did not show substantial
548 changes (< 2%) despite temporal variation in water availability and cambial activity.
549 This consistency indicates that the contribution of E_A to R_S was constant and high
550 during the vegetative period, once leaves had expanded, and suggests that E_A may be a

551 good estimator of R_S at large temporal scales in *Q. pyrenaica* and perhaps other
552 drought-adapted species (Rodríguez-Calcerrada et al. 2014). Low transpiration rates
553 characteristic of sub-Mediterranean species, together with low resistance to radial CO_2
554 diffusion and low internal $[\text{CO}_2]$, may explain the strong coupling between E_A and R_S in
555 this study. Nonetheless, despite the small contribution of F_T to R_S on a daily basis, we
556 emphasize that the influence of internal transport of CO_2 across interconnected roots
557 and stems of *Q. pyrenaica* on R_S (with F_T accounting up to 25% of R_S in daytime) is
558 important to our understanding of the fate of respired CO_2 .

559 *Conclusions*

560 Relative to previous reports, xylem $[\text{CO}_2]$ was low in *Q. pyrenaica* stems. Due to low
561 $[\text{CO}_2]$, F_T did not account for more than 10% of total R_S on a daily basis, suggesting that
562 E_A may be a suitable estimator of R_S for this species, and perhaps others, under drought
563 conditions. Low stem $[\text{CO}_2]$ and F_T was related to high permeability of phloem and bark
564 tissues to diffusion of CO_2 that appeared to be driven by water deficit, as the resistance
565 to radial CO_2 diffusion decreased across the growing season along with decreasing
566 midday water potential. Variation in the resistance to radial CO_2 diffusion in relation to
567 environmental conditions might be a currently overlooked factor that could be important
568 to our understanding of stem respiration.

569 **Acknowledgements**

570 We are grateful to Javier Donés for economic and logistical support. We also thank
571 Guillermo González, Elena Zafra, Paula Guzman, Aida Rodríguez, Jose Carlos
572 Miranda, Manuel Iglesias, Rosa Ana López, Eva María Miranda, César Otero and
573 Ricardo Álvarez for their inestimable help with field work.

574 **Conflict of interest**

575 None declared.

576 **Funding**

577 This work was funded by the Comunidad de Madrid through CAM P2009/AMB-1668
578 and P2013/MAE-2760 projects. Roberto Salomón was supported by a Ph.D. scholarship
579 from the Universidad Politécnica de Madrid. Jesús Rodríguez-Calcerrada was supported

580 by a Juan de la Cierva contract from the Spanish Ministry of Economy and
581 Competitiveness.

582

583 **References**

- 584 Acosta M, Pavelka M, Pokorný R (2008) Seasonal variation in CO₂ efflux of stems and
585 branches of Norway spruce trees. *Ann Bot* 101:469–477.
- 586 Amthor J (2000) The McCree–de Wit–Penning de Vries–Thornley respiration
587 paradigms: 30 years later. *Ann Bot* 86:1–20.
- 588 Angert A, Muhr J, Negron Juarez R, Alegria Muñoz W, Kraemer G, Ramirez Santillan
589 J, Barkan E, Maze S, Chambers JQ, Trumbore SE (2012) Internal respiration of
590 Amazon tree stems greatly exceeds external CO₂ efflux. *Biogeosciences Discuss*
591 9:11443–11477.
- 592 Araki MG, Utsugi H, Kajimoto T, Han Q, Kawasaki T, Chiba Y (2010) Estimation of
593 whole-stem respiration, incorporating vertical and seasonal variations in stem CO₂
594 efflux rate, of *Chamaecyparis obtusa* trees. *J For Res* 15:115–122.
- 595 Aubrey DP, Teskey RO (2009) Root-derived CO₂ stream rivals soil CO₂ efflux. *New*
596 *Phytol* 184:35–40.
- 597 Barbaroux C, Bréda N (2002) Contrasting distribution and seasonal dynamics of
598 carbohydrate reserves in stem wood of adult ring-porous sessile oak and diffuse-
599 porous beech trees. *Tree Physiol* 22:1201–1210.
- 600 Bloemen J, Teskey RO, McGuire M a., Aubrey DP, Steppe K (2015) Root xylem CO₂
601 flux: an important but unaccounted-for component of root respiration. *Trees*
602 DOI:10.1007/s00468–015–1185–4.
- 603 Bowman WP, Barbour MM, Turnbull MH, Tissue DT, Whitehead D, Griffin KL (2005)
604 Sap flow rates and sapwood density are critical factors in within- and between-tree
605 variation in CO₂ efflux from stems of mature *Dacrydium cupressinum* trees. *New*
606 *Phytol* 167:815–828.
- 607 Brito P, Morales D, Wieser G, Jiménez MS (2010) Spatial and seasonal variations in
608 stem CO₂ efflux of *Pinus canariensis* at their upper distribution limit. *Trees*
609 24:523–531.
- 610 Bužková R, Acosta M, Dařenová E, Pokorný R, Pavelka M (2015) Environmental
611 factors influencing the relationship between stem CO₂ efflux and sap flow. *Trees*
612 24:285–296.
- 613 Cerasoli S, McGuire MA, Faria J, Mourato M, Schmidt M, Pereira JS, Chaves MM,
614 Teskey RO (2009) CO₂ efflux, CO₂ concentration and photosynthetic re-fixation in
615 stems of *Eucalyptus globulus* (Labill.). *J Exp Bot* 60:99–105.
- 616 Chase WW (1934) The composition, quantity and physiological significance of gases in
617 tree stems. Minnesota Agricultural Experiment Station Technical Bulletin 99,
618 Minnesota, USA.

- 619 Corcuera L, Camarero JJ, Sisó S, Gil-Pelegrín E (2006) Radial-growth and wood-
620 anatomical changes in overaged *Quercus pyrenaica* coppice stands: functional
621 responses in a new Mediterranean landscape. *Trees* 20:91–98.
- 622 Courty PE, Bréda N, Garbaye J (2007) Relation between oak tree phenology and the
623 secretion of organic matter degrading enzymes by *Lactarius quietus*
624 ectomycorrhizas before and during bud break. *Soil Biol Biochem* 39:1655–1663.
- 625 Damesin C, Ceschia E, Le Goff N, Ottorini JM, Dufrêne E (2002) Stem and branch
626 respiration of beech: from tree measurements to estimations at the stand level. *New*
627 *Phytol* 153:159–172.
- 628 DesRochers A, Lieffers VJ (2001) The coarse-root system of mature *Populus*
629 *tremuloides* in declining stands in Alberta, Canada. *J Veg Sci* 12:355–360.
- 630 Edwards NT, Hanson PJ (1996) Stem respiration in a closed-canopy upland oak forest.
631 *Tree Physiol* 16:433–9.
- 632 Etzold S, Zweifel R, Ruehr N (2013) Long-term stem CO₂ concentration measurements
633 in Norway spruce in relation to biotic and abiotic factors. *New Phytol* 197:1173–
634 1184.
- 635 Gansert D, Burgdorf M (2005) Effects of xylem sap flow on carbon dioxide efflux from
636 stems of birch (*Betula pendula* Roth). *Flora* 200:444–455.
- 637 Granier A (1985) Une nouvelle méthode pour la mesure du flux de sève brute dans le
638 tronc des arbres. *Ann For Sci* 42:193–200.
- 639 Guidolotti G, Rey A, D’Andrea E, Matteucci G, De Angelis P (2013) Effect of
640 environmental variables and stand structure on ecosystem respiration components
641 in a Mediterranean beech forest. *Tree Physiol* 33:960–72.
- 642 Hölttä T, Kolari P (2009) Interpretation of stem CO₂ efflux measurements. *Tree Physiol*
643 29:1447–1456.
- 644 Hothorn T, Bretz F, Westfall P (2008) Simultaneous inference in general parametric
645 models. *Biometrical J* 50:346–363.
- 646 Lavigne MB, Little CHA, Riding RT (2004) Changes in stem respiration rate during
647 cambial reactivation can be used to refine estimates of growth and maintenance
648 respiration. *New Phytol* 162:81–93.
- 649 Maier CA, Clinton BD (2006) Relationship between stem CO₂ efflux, stem sap velocity
650 and xylem CO₂ concentration in young loblolly pine trees. *Plant, Cell Environ*
651 29:1471–1483.
- 652 Maier CA, Johnsen KH, Clinton BD, Ludovici KH (2010) Relationships between stem
653 CO₂ efflux, substrate supply, and growth in young loblolly pine trees. *New Phytol*
654 185:502–513.

- 655 Manuel Valdés C, Rojo y Alboreca A (1993) Valsaín forest in the XVIII century: an
656 example of forest management in the pre-industrial era. *Investig Agrar Sist y Recur*
657 *For* 3:217–229.
- 658 Maseyk K, Grünzweig JM, Rotenberg E, Yakir D (2008) Respiration acclimation
659 contributes to high carbon-use efficiency in a seasonally dry pine forest. *Glob*
660 *Chang Biol* 14:1553–1567.
- 661 McGuire MA, Teskey RO (2004) Estimating stem respiration in trees by a mass balance
662 approach that accounts for internal and external fluxes of CO₂. *Tree Physiol*
663 24:571–578.
- 664 Nobel PS (1999) *Physicochemical and environmental plant physiology*. Academic press,
665 San Diego, CA, USA.
- 666 Pinheiro J, Bates D, DebRoy S, Sarkar D, R Core Team (2015) nlme: Linear and
667 nonlinear mixed effects models. R Packag version 3.1-122
- 668 Rambal S, Lempereur M, Limousin JM, Martin-StPaul NK, Ourcival JM, Rodríguez-
669 Calcerrada J (2014) How drought severity constrains gross primary production
670 (GPP) and its partitioning among carbon pools in a *Quercus ilex* coppice?
671 *Biogeosciences* 11:6855–6869.
- 672 Rodríguez-Calcerrada J, López R, Salomón R, Gordaliza G, Valbuena-Carabaña M,
673 Oleksyn J, Gil L (2015) Stem CO₂ efflux in six co-occurring tree species:
674 underlying factors and ecological implications. *Plant, Cell Environ* 38:1104–1115.
- 675 Rodríguez-Calcerrada J, Martin-StPaul NK, Lempereur M, Ourcival JM, Rey MC,
676 Joffre R, Rambal S (2014) Stem CO₂ efflux and its contribution to ecosystem CO₂
677 efflux decrease with drought in a Mediterranean forest stand. *Agric For Meteorol*
678 195-196:61–72.
- 679 Ryan MG, Cavaleri MA, Almeida AC, Penchel R, Senock RS, Luiz Stape J (2009)
680 Wood CO₂ efflux and foliar respiration for Eucalyptus in Hawaii and Brazil. *Tree*
681 *Physiol* 29:1213–1222.
- 682 Salomón R, Valbuena-Carabaña M, Gil L, González-Doncel I (2013) Clonal structure
683 influences stem growth in *Quercus pyrenaica* Willd. coppices: Bigger is less
684 vigorous. *For Ecol Manage* 296:108–118.
- 685 Salomón R, Valbuena-Carabaña M, Rodríguez-Calcerrada J, Aubrey D, McGuire M,
686 Teskey R, Gil L, González-Doncel I (2015) Xylem and soil CO₂ fluxes in a
687 *Quercus pyrenaica* Willd. coppice: Root respiration increases with clonal size. *Ann*
688 *For Sci*. DOI:10.1007/s13595-015-0504-7.
- 689 Saveyn A, Steppe K, Lemeur R (2007a) Daytime depression in tree stem CO₂ efflux
690 rates: Is it caused by low stem turgor pressure? *Ann Bot* 99:477–485.
- 691 Saveyn A, Steppe K, Lemeur R (2007b) Drought and the diurnal patterns of stem CO₂

- 692 efflux and xylem CO₂ concentration in young oak (*Quercus robur*). *Tree Physiol*
693 27:365–374.
- 694 Saveyn A, Steppe K, McGuire MA, Lemeur R, Teskey RO (2008) Stem respiration and
695 carbon dioxide efflux of young *Populus deltoides* trees in relation to temperature
696 and xylem carbon dioxide concentration. *Oecologia* 154:637–49.
- 697 Sorz J, Hietz P (2006) Gas diffusion through wood: Implications for oxygen supply.
698 *Trees* 20:34–41.
- 699 Steppe K, Saveyn A, McGuire MA, Lemeur R, Teskey RO (2007) Resistance to radial
700 CO₂ diffusion contributes to between-tree variation in CO₂ efflux of *Populus*
701 *deltoides* stems. *Funct Plant Biol* 34:785–792.
- 702 Stockfors J, Linder S (1998) Effect of nitrogen on the seasonal course of growth and
703 maintenance respiration in stems of Norway spruce trees. *Tree Physiol* 18:155–
704 166.
- 705 Sun H, Aubrey DP, Teskey RO (2011) A simple calibration improved the accuracy of the
706 thermal dissipation technique for sap flow measurements in juvenile trees of six
707 species. *Trees* 26:631–640.
- 708 Tarvainen L, Rantfors M, Wallin G (2014) Vertical gradients and seasonal variation in
709 stem CO₂ efflux within a Norway spruce stand. *Tree Physiol* 34:488–502.
- 710 Teskey RO, McGuire MA (2002) Carbon dioxide transport in xylem causes errors in
711 estimation of rates of respiration in stems and branches of trees. *Plant, Cell*
712 *Environ* 25:1571–1577.
- 713 Teskey RO, McGuire MA (2007) Measurement of stem respiration of sycamore
714 (*Platanus occidentalis* L.) trees involves internal and external fluxes of CO₂ and
715 possible transport of CO₂ from roots. *Plant, Cell Environ* 30:570–579.
- 716 Teskey RO, Saveyn A, Steppe K, McGuire MA (2008) Origin, fate and significance of
717 CO₂ in tree stems. *New Phytol* 177:17–32.
- 718 Trumbore SE, Angert A, Kunert N, Muhr J, Chambers JQ (2013) What’s the flux?
719 Unraveling how CO₂ fluxes from trees reflect underlying physiological processes.
720 *New Phytol* 197:353–355.
- 721 Ubierna N, Kumar AS, Cernusak LA, Pangle RE, Gag PJ, Marshall JD (2009) Storage
722 and transpiration have negligible effects on δ¹³C of stem CO₂ efflux in large
723 conifer trees. *Tree Physiol* 29:1563–1574.
- 724 Valbuena-Carabaña M, Gil L (2013) Genetic resilience in a historically profited root
725 sprouting oak (*Quercus pyrenaica* Willd.) at its southern boundary. *Tree Genet*
726 *Genomes* 9:1129–1142.
- 727 Valbuena-Carabaña M, González-Martínez SC, Gil L (2008) Coppice forests and

728 genetic diversity: A case study in *Quercus pyrenaica* Willd. from Central Spain.
729 For Ecol Manage 254:225–232.

730 Waring R, Landsberg J, Williams M (1998) Net primary production of forests: a
731 constant fraction of gross primary production? Tree Physiol 18:129–134.

732 Wertin TM, Teskey RO (2008) Close coupling of whole-plant respiration to net
733 photosynthesis and carbohydrates. Tree Physiol 28:1831–1840.

734 Xu M, DeBiase TA, Qi Y (2000) A simple technique to measure stem respiration using a
735 horizontally oriented soil chamber. Can J For Res 30:1555–1560.

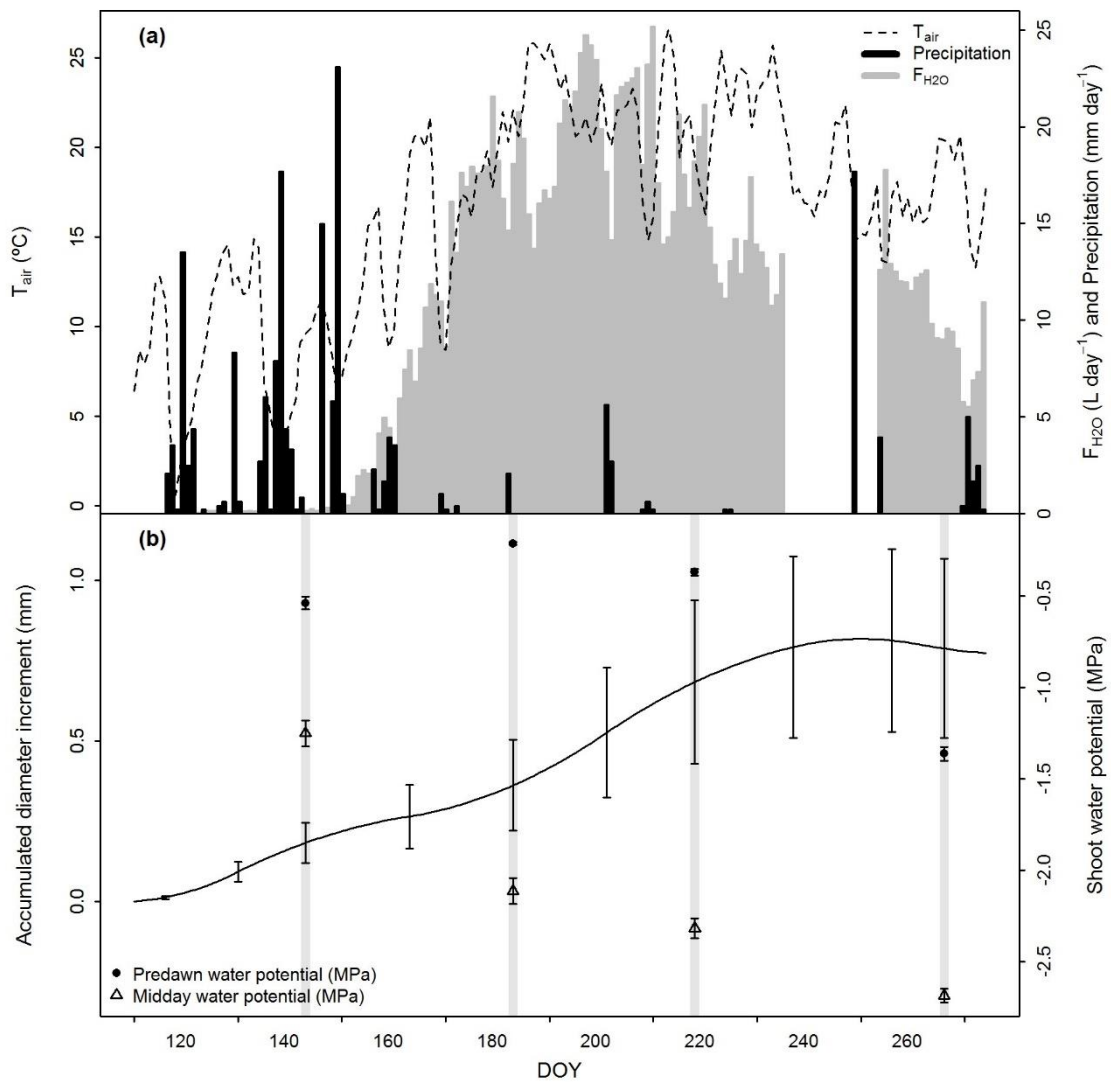
736 Yang Q, Xu M, Chi Y, Zheng Y, Shen R, Li P, Dai H (2012) Temporal and spatial
737 variations of stem CO₂ efflux of three species in subtropical China. J Plant Ecol
738 5:229–237.

739 Zach A, Horna V, Leuschner C (2010) Diverging temperature response of tree stem CO₂
740 release under dry and wet season conditions in a tropical montane moist forest.
741 Trees 24:285–296.

742 Zeppel MJB, Harrison SP, Adams HD, Kelley DI, Li G, Tissue DT, Dawson TE,
743 Fensham R, Medlyn BE, Palmer A, West AG, McDowell NG (2015) Drought and
744 resprouting plants. New Phytol 206:583–589.

745

746 Figure 1. Daily air temperature (T_{air}), precipitation, and average sap flow per tree (F_{H2O})
 747 (a); and accumulated diameter increment and predawn and midday shoot water potential
 748 (b) across the growing season in an experimental plot of *Quercus pyrenaica*. Stem
 749 growth began before budburst and leaf expansion and ceased at the end of the dry
 750 season before first autumn rains (DOY 249). Four measurement campaigns are depicted
 751 by grey vertical bars. The gap in the F_{H2O} series from DOY 236-253 corresponds to the
 752 theft of the power supply on DOY 236.

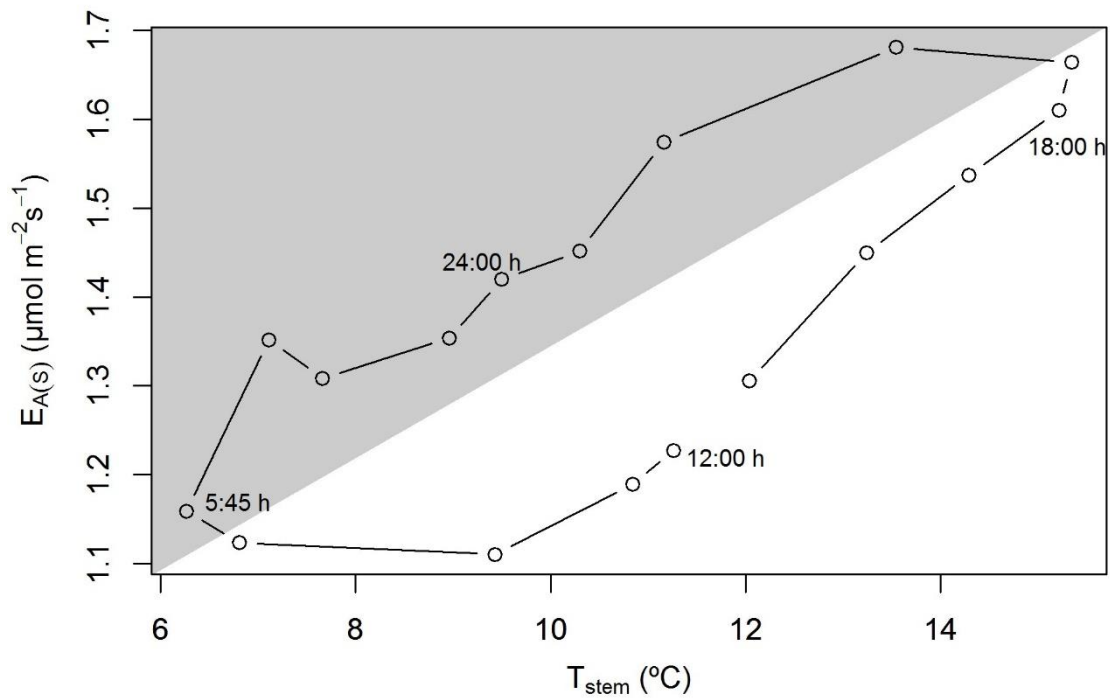


753

754

755

756 Figure 2. Example of hysteresis in the relationship between stem temperature (T_{stem}) and
757 stem CO_2 efflux on a surface basis ($E_{A(S)}$). Measurements started at midday and follow a
758 counterclockwise pattern. Shaded area indicates nighttime. In the example, for a given
759 temperature, $E_{A(S)}$ was higher at nighttime than at daytime at negligible sap flow rates
760 (DOY 143-144, during budburst). Similar hysteresis was observed throughout the
761 course of the experiment.

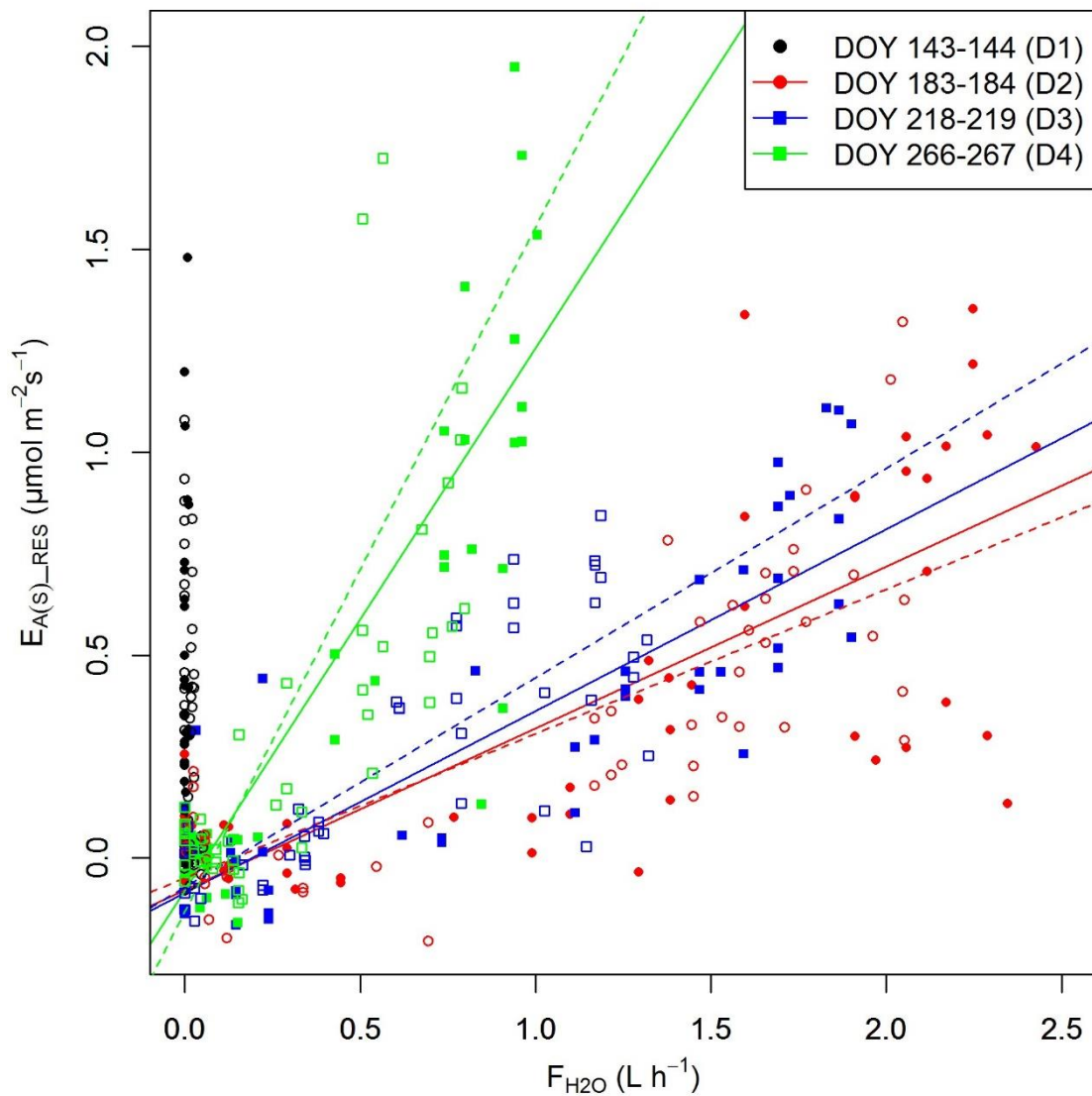


762

763

764

765 Figure 3. Residual stem CO₂ efflux ($E_{A(S_RES)}$) regressed against sap flow (F_{H_2O}).
766 Residual stem CO₂ efflux was calculated as the difference between predicted (from the
767 nighttime relationship between efflux and temperature, Eq. 1) and measured CO₂ efflux
768 during the daytime. Significant regression lines ($P < 0.05$) per stem and date are
769 depicted. On the leafless measurement date (D1), sap flow and $E_{A(S_RES)}$ were not
770 related ($P = 0.319$), whereas positive relationships ($P < 0.001$) were found on the
771 remaining dates after leaf expansion ($R^2 = 0.604, 0.699, 0.618$ for D2, D3, and D4,
772 respectively). The slopes of these relationships were similar on D2 and D3 ($P = 0.378$),
773 whereas slopes on D2 and D3 were different than the slope on D4 ($P < 0.001$).

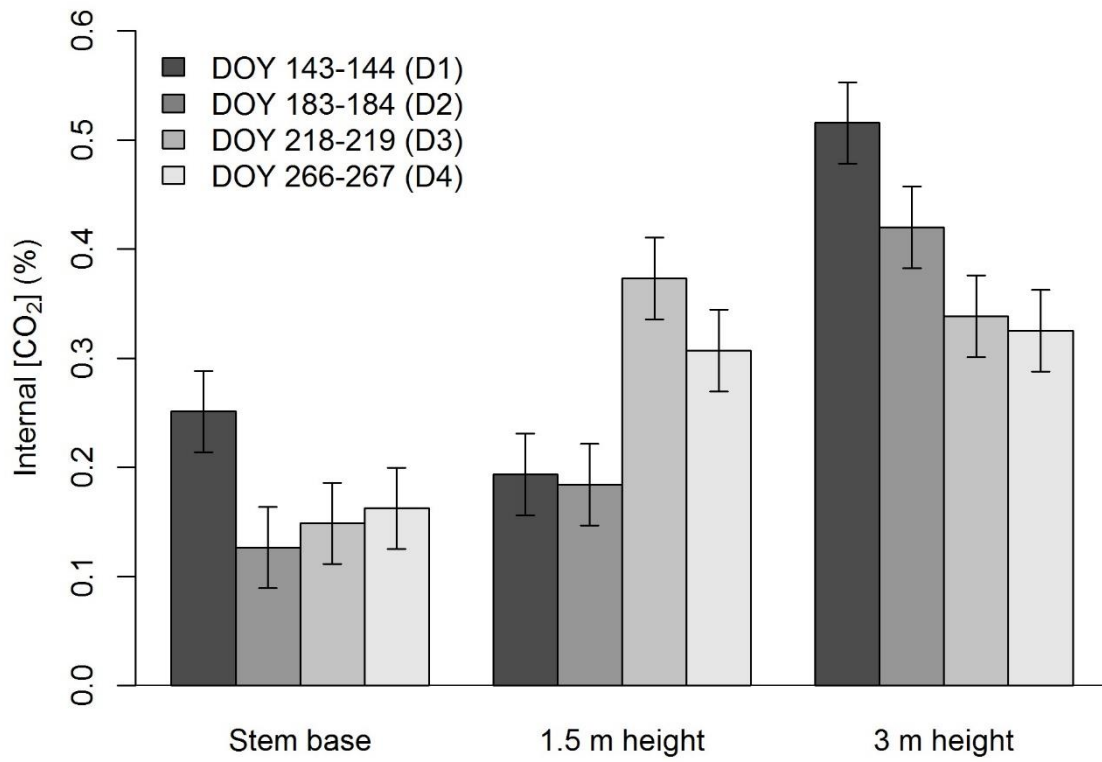


774

775

776

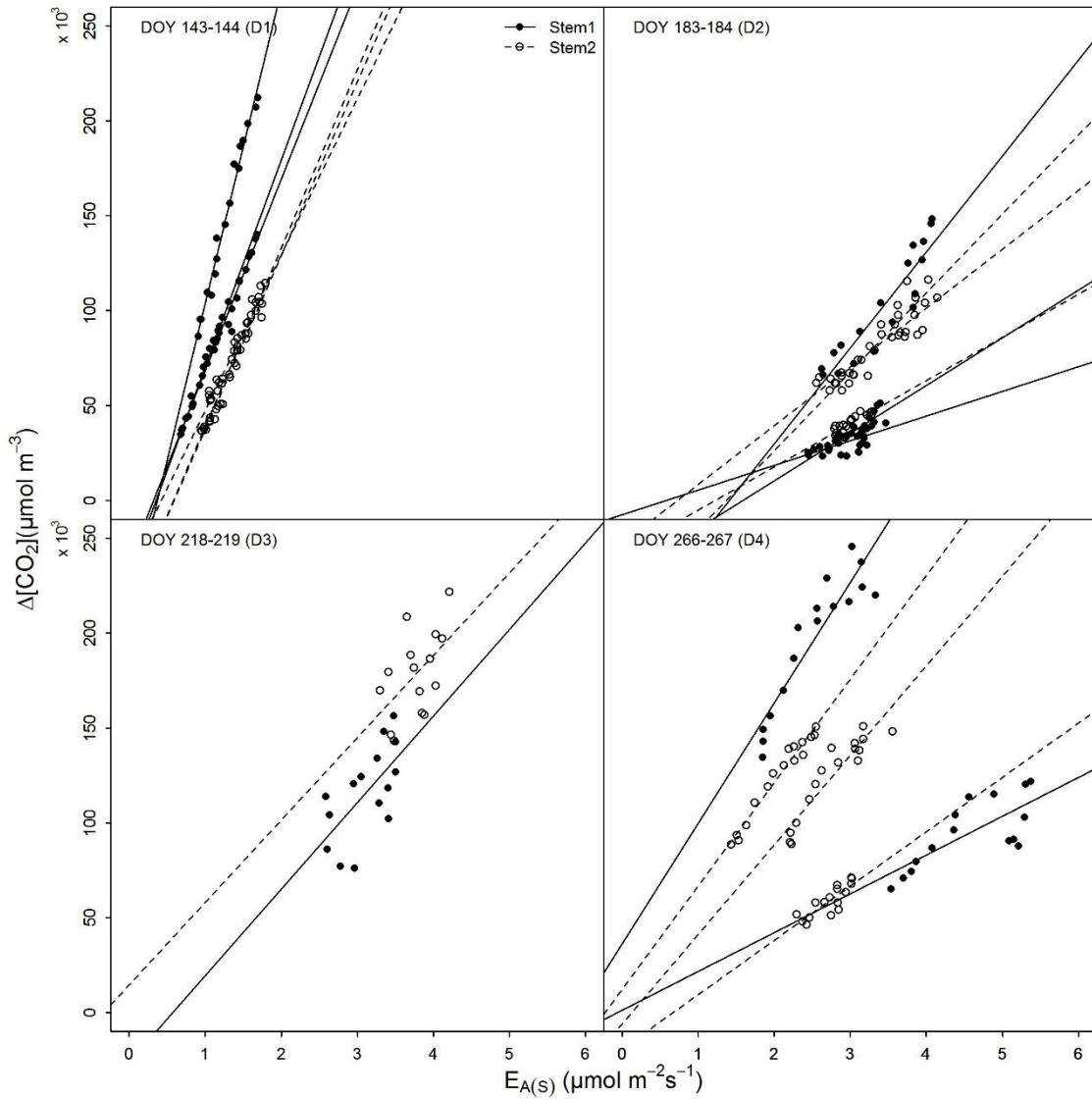
777 Figure 4. Mean internal [CO₂] across the growing season at three stem heights. Mean
778 internal [CO₂] was calculated for the two stems on which measurements were made at
779 different heights.



780

781

783 Figure 5. CO₂ concentration gradient between xylem and atmosphere ($\Delta[\text{CO}_2]$) in
 784 relation to stem CO₂ efflux to the atmosphere ($E_{A(S)}$) on four measurement dates across
 785 the growing season. The slope of this relationship represents stem resistance to radial
 786 CO₂ diffusion. Measurements at three heights on two *Quercus pyrenaica* stems are
 787 depicted by open and closed circles. Only significant regressions ($P < 0.05$) are shown.
 788 Resistance to radial CO₂ diffusion was highest on the first measurement date ($P <$
 789 0.001).

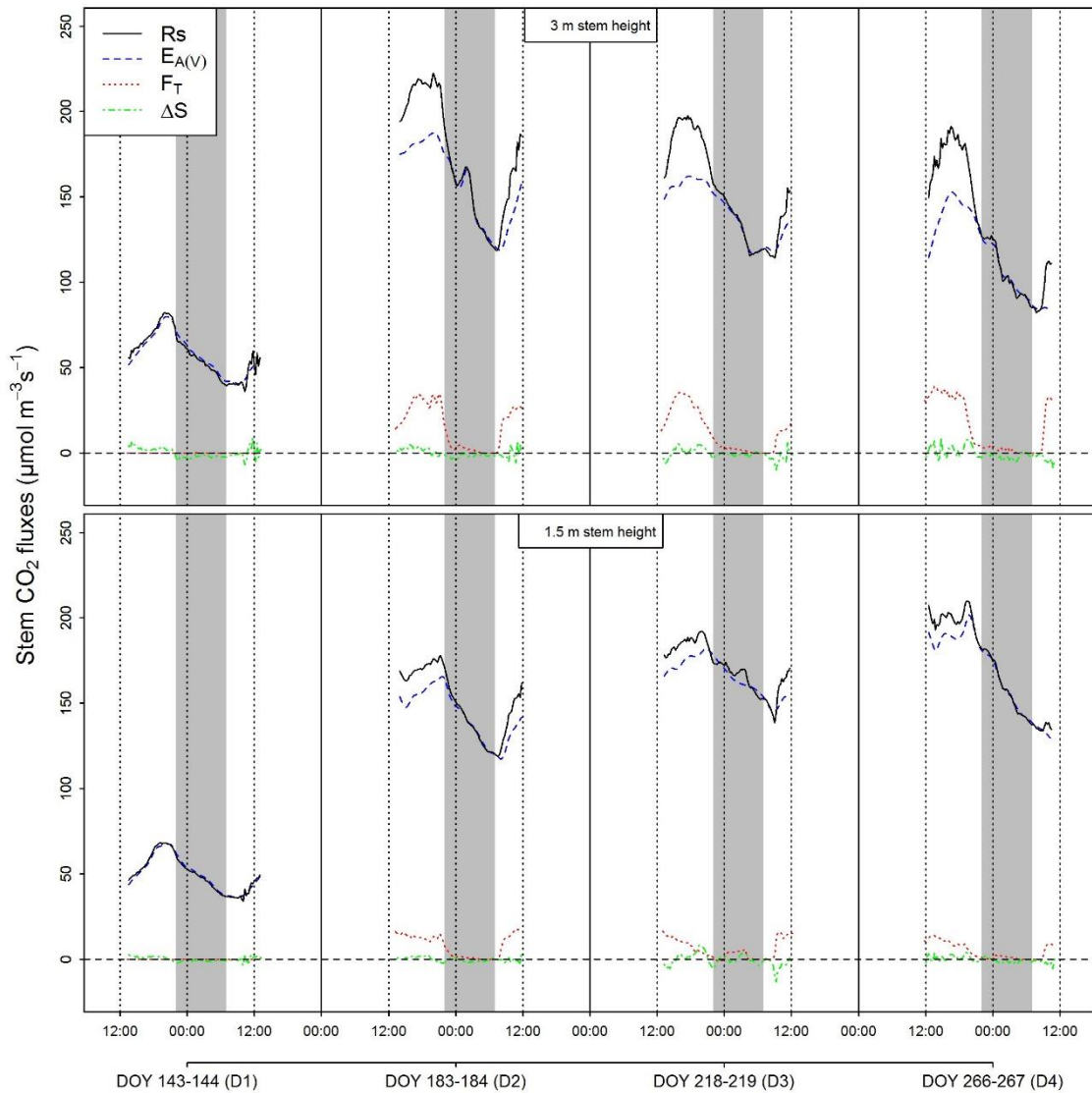


790

791

792

793 Figure 6. Diel variations in stem respiration (R_s) and its components - stem CO_2 efflux
794 to the atmosphere ($E_{A(V)}$), internal CO_2 transport through xylem (F_T) and CO_2 storage
795 flux (ΔS) - on four dates over the growing season. Mass balance at 1.5 m stem height
796 calculated from average of two stems. Mass balance at 3 m stem height calculated for
797 one stem due to NDIR probe failure in the second stem at two dates. Shaded areas
798 indicate nighttime.



799

800